International Journal of Research in Advent Technology, Vol.7, No.5, May 2019
E-ISSN: 2321-9637
Available online at www.ijrat.org

Enhanced Photocatalytic performance of activated carbon-SiO_2 Nanocomposite on the removal of Methylene blue dye from aqueous solution

S.K Nirmala[1], P.Rajesh[1*], R. Venckatesh[2], Rajeswari sivaraj[2] and M. Ezhil Inban[3]
[1]*Department of Chemistry, Government Arts College, Coimbatore - 641018, Tamil Nadu, India*
[2]*Department of Chemistry, Government Arts College, Udumalpet - 642126, TamilNadu, India*
[3]*Department of Physics, Government Arts College, Coimbatore- 641 018, Tamil Nadu, India*
Email : nirmala.sathy2010@gmail.com[1], gacchemistryrajesh@gmail.com[2], rvenckat@gmail.com[3], rajeshwarishivaraj@gmail.com[4]

Abstract- Activated carbon (AC) - SiO2 nanocomposite was synthesized using microwave assisted sol-gel method and utilized for the photocatalytic degradation of Methylene blue dye in aqueous solution. Surface morphology and bulk composition of the composite was obtained using electron microscopy with energy dispersive X-ray analysis. The SEM and TEM image of AC- SiO2 shows the presence of spherical particles with an average size around 40 nm. The data of X-ray diffraction shows the incorporation of carbon into the SiO_2 matrix. The crystal structure and elemental composition was analyzed by Fourier transform spectroscopy. The photocatalytic experiments were performed with aqueous solution of Methylene blue for 2 h irradiation. Direct photolysis of AC-SiO_2 contributed 84.5% decomposition in solar radiation for the optimized concentration of Methylene blue.

Keywords: Photocatalysis; Activated carbon; Silica; Nanocomposite; Methylene blue

1. INTRODUCTION

Nowadays, Dyes and pigments are the most significant pollutants that are extremely dangerous on water resources .During production and usage many contaminations enter into the environment. The degradation of these chemicals into harmless compounds is challenging The wastewater that enters the environment without purification affects the water ecosystem Therefore, purification of wastewater is necessary before it is discharged. Many physical and chemical methods are being used for this purpose, which include reverse osmosis, adsorption, precipitation, ion exchange and coagulation [1]. These methods only transfer pollution from one phase to another and concentrate them. Recently, photochemistry of nano semiconductor particles has been one of the fastest growing research areas in wastewater treatment. The interest in these small semiconductor particles is due to their unique photo physical and photocatalytic properties. Heterogeneous photocatalysis is an interesting technique for environmental remediation, where semiconductor metal oxides are used as photo catalysts. When organic dyes are decomposed by heterogeneous catalytic reactions, the dye containing wastewater is adsorbed on the surface of the photo catalysts. The chemical bonds are broken down and formed and finally small organic molecules are released as decomposed products [2, 3].Silica is suitable in many areas such as ceramics, glass industries, photovoltaic cells and it is also used as catalytic support [4, 5]. However, SiO_2 exhibits good catalytic and photocatalytic activities [6, 7]. Recently, bi-metal and tri-metal doped SiO_2 has become of interest in promoting photocatalytic reactions under UV- light irradiation [8, 9]. Activated carbon is an excellent adsorbent of countless pollutants, due to its ability to adsorb the dye molecules and then release them onto the surface of the catalysts. The intermediates produced during degradation can be also adsorbed by AC and then further oxidized [10, 11]. The sol-gel technique is most commonly employed for the synthesis of silica as well as metal and carbon doped SiO_2 core-shell matrices and composites [12]. Various supported materials have been proposed for degradation of several dye molecules [13, 14].

In this work microwave, assisted sol-gel route has been utilized for synthesis of AC-SiO_2 nanocomposite. The synthesized samples were characterized by UV-Vis, SEM with EDX, XRD, FT-IR. The composite was utilized to explore the photocatalytic properties of the synthesized AC–SiO_2 nanocomposites using Methylene blue dye under solar radiation.

2. EXPERIMENTAL DETAILS

2.1. Biomass preparation

Coccinia indica bark was washed with tap water, then rinsed with double-de-ionized water and dried first in the sun light for 7 days. Resulting dried bark was cut into small pieces and used for further studies.

2.2. Impregnation using sulfuric acid (H_2SO_4)

In a 5L trough 500 g of *Coccinia indica* bark was contacted 500 ml sulphuric acid during a fixed period of impregnation time, temp [15].The impregnated samples were recovered by filtration and dried at room temperature for 2 days. They were calcined in a muffle furnace for 3 h. Later the activated carbon was rinsed with double-ionized water until pH 6, dried in hot air oven for 4 h, and used for further studies.

2.3. Preparation of AC-SiO_2 nanoparticles

SiO_2 sol was prepared by using Silicic acid with Tetrahydrofuran in the ratio of 1:2. Isopropanol solution was added to the above mixture with continuous stirring of the suspension for 2h and irradiated in microwave oven for 30 min. The prepared gel was mixed with weighed amount of activated carbon (AC) with continuous stirring for 1h. The reaction products were filtered, washed with copius amount deionized water and dried in hot air oven at 80^oC.

The cationic dye, Methylene blue Methylene blue was purchased from Sigma-Aldrich. All the above reagents were analytical grade without any additional purification. Deionized water was used throughout the reactions and synthesis process. Besides, all the experimental tests were performed at room temperature.

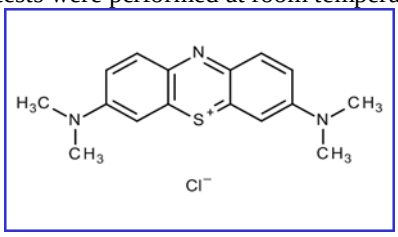

Fig.1. Structure of Methylene blue Mol.F $C_{16}H_{18}ClN_3S$

2.4. Characterization

The prepared AC-SiO_2 nanocomposites was characterized for the crystalline structure using D8 Advance X-ray diffraction meter (Bruker AXS, Germany) at room temperature, operating at 30 kV and 30 mA, using Cu *Kα* radiation (λ = 0.15406 nm). The crystal size was calculated by Scherer's formula. Surface morphology was studied by using SEM-EDS (Model JSM 6390LV, JOEL, USA), UV–Vis diffuse reflectance spectra was recorded with a Carry 5000 UV-Vis-NIR spectrophotometer (Varian, USA) and FT-IR spectra were measured on an AVATAR 370-IR spectrometer (Thermo Nicolet, USA) with a wave number range of 4000 to 400 cm^{-1}.

2.5. Photocatalytic activity

The photocatalytic activity of the AC-SiO_2 was studied under solar radiations. In a typical experiment, aqueous suspensions of Methylene blue dye solutions (20, 40, 60, 80 mg/L) and 0.1 g of the AC - photo catalysts were placed in reaction bottles. Prior to irradiation, the suspension was stirred magnetically to ensure an adsorption/desorption equilibrium. At regular intervals of given irradiation time the suspension were withdrawn, filtered and measured spectrophotometrically (615 nm). The effect of catalyst load was studied using (0.5 to 1.0g) of the adsorbent and pH study was carried out from 2 -12 for all the four concentrations of the dye.

3. RESULTS AND DISCUSSION

3.1. Characterization of the photocatalyst

The ultraviolet-visible spectrum of Methylene blue dye shows strong absorption bands in the visible spectral region with a maximum at 662 nm. The SEM images of AC- SiO_2 show that the nanoparticles possess an almost spherical shape with homogenous distribution of Si particles throughout the amorphous carbon. AC- SiO_2 shows an average particle size of 35 - 40 nm [2a]. Additionally, the AC- SiO_2 agglomerates possess a rough and porous surface, resulting in an increased surface area. which suggests that these nanocomposite could be chemically reactive, therefore suitable for photocatalytic applications. EDX analysis confirms the presence of Si, C and O in Ac-SiO_2 with peaks for the elements Si, O and C appearing at 1.7 keV, 0.5 keV and 0.3 keVs,. TEM image of the sample [2b] demonstrates that the sample is entirely amorphous Furthermore, the mesoporous SiO_2 has a three dimensionally interconnected and disordered globular-like mesopore structure and the size of mesopore is almost homogeneous. The FTIR spectrum [2 c] reports absorption peak near 1100 cm^{-1}, which corresponds to the Si–O–Si stretching vibrations. The broad band around 3403 cm^{-1} is attributed to O–H stretching and the peak near 1630 cm^{-1} to O–H bending which is related to physically absorbed moisture. It is considered that the dopant Si enhanced the water absorption and the more OH were formed. Thereby, the photo-catalytic activity of Ac - $SiO_2$was increased [16]. The XRD results show broad peak at 2θ = 48.0, 54.0 and 62.0 corresponding to the (200), (211) and (204) crystal planes reflection of anatase. [17, 18], The XRD of the modified sample shows hump at 2 theta range (40-50) deg., this means that the composite is highly disordered and amorphous in nature.

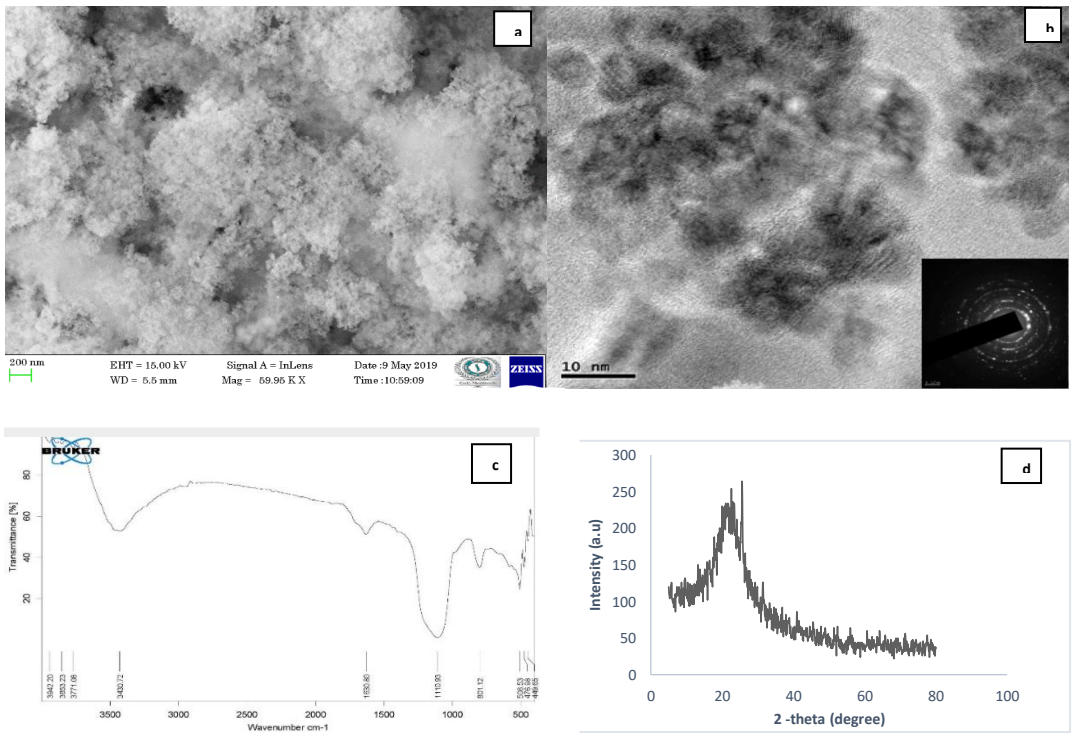

Fig. 2. (a) SEM (b) TEM (c)FTIR (d) XRD image of AC- SiO_2 carbon

3.2. Photocatalytic studies

3.2.1. Initial dye concentration

Fig. 3a shows the effect of initial dye concentration on photo degradation by the Ac-SiO_2 nanocomposite. The results show that the decomposition of MB decreased with increasing initial dye concentrations of the dye from 20 to 80 mg/L. The visible light enters more easily through the solution to irradiate the Ac-SiO_2 when the initial dye concentration is lower.

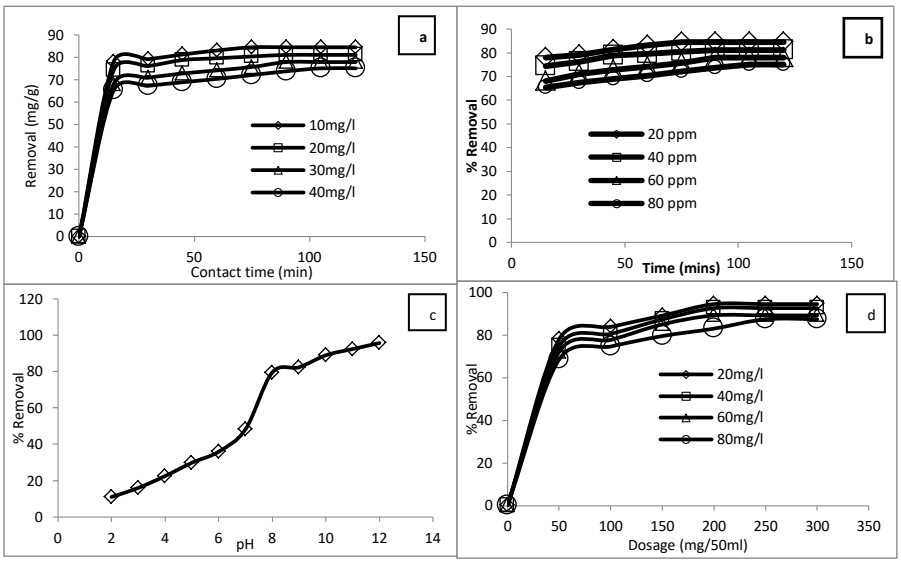

Fig.3. Adsorption and photocatalytic oxidation effects of (a) concentration, (b) contact time (c) dose (d) pH for MB adsorption onto AC-SiO_2 nanocomposite

The photonic efficiency increased with decreasing initial dye concentration, which may be possibly attributed to the increase of collision frequency between dye molecules and photons. With increase in the concentration, large amount of dyes are adsorbed on the composite, which prevented from dye molecule reaction with free radical and electron holes. Hence, at higher dye concentrations, photonic efficiency is decreased [19, 20].However, at high concentration of MB, lower adsorption efficiency was reported due to saturation of active sites on the adsorbent's surface [21, 22]. This suggests that as the initial concentration of the dye increases, the requirement of catalyst surface needed for the decomposition also increases. Since irradiation time and amount of catalyst are constant, the –OH radical formed on the surface of AC-SiO_2 is also constant and hence the relative number of free radicals attacking the dye molecules decreases with increasing amount of the catalyst [23].

3.2.2. Effect of contact time

The photocatalytic percent degradation of Methylene blue against irradiation time is shown in Fig. 3b. Results show that a linear relationship of dye removal with increase of time. In case of Methylene blue, a maximum of 84.5% degradation was observed (20mg/L).When time increases more and lighter energy falls on the catalyst surfaces, which increases the formation of photo-excited species and enhances the photocatalytic activity [24]. Moreover, the higher surface area and small particle size of the modified catalyst also contribute to the higher activity and hence increased absorption and decomposition of the dye molecules.

3.2.3. Effect of catalyst amount

Fig. 3c. shows the effect of nanocomposite on Methylene blue dye removal. The results show that the percent degradation of the dye increases with increase in the amount of the catalyst (50- 300 mg/50ml). This indicated that the active sites provided for the adsorption of substrate on the catalyst surface is limited to catalyst amount. The minimum percentage decomposition at lower AC-SiO_2 loading can be attributed to the fact that more light is transmitted through the suspension, which is not utilized in the photocatalytic reaction. The increase in the degradation efficiency of the dye with an increase in the catalyst load may be attributed to an increase in the active sites available on the catalyst surface for the reaction, which in turn increases the rate of radical formation [25-27].

3.2.4. Effect of pH

The pH is the important factor which controls the adsorption process especially for cationic dyes. The effect of pH of the dye solution on the removal of MB was determined at fixed concentration 20-80 mg/L of dyes over a pH range of (2.0 to 12) as shown in Fig.3d. The maximum adsorption of the dyes was observed above pH 4.0. Lower adsorption of dyes at low pH is probably due to the presence of H^+ ions competing with the cationic groups on the dye for adsorption sites varies potential of catalyst reactions. As surface charge density decrease with an increase in the solution pH, the electrostatic repulsion between the positively charged MB and nanocomposite is lowered, this may result in an increase in the rate of adsorption molecules [28]. An increased diffusion process facilitates dye attachment at the active sites of the adsorbents. The figure clearly reveal that with further increase in pH from 8 to 12, the adsorption process attains equilibrium. Simple conditions favour adsorption of dyes and pH 8 was found optimum for the nanocomposite.

3.3. Adsorption Kinetics study

Many attempts have been made to formulate a general expression describing the kinetics of sorption on solid surfaces for liquid– solid phase sorption systems. Lagergren first represented the pseudo-first order equation for the adsorption of oxalic acid and malonic acid onto charcoal. The Lagergren kinetic model has been used to investigate the mechanism of sorption and potential rate controlling steps such as mass transport and chemical reaction processes

3.3.1. Pseudo-first order equation

The pseudo-first order equation of Lagergren is generally expressed as follows:

$$\log(q_e - q_t) = (\log q_e - (K_{ad}/2.303) \times t \quad (1)$$

where q_e is the amount of dye adsorbed (mg/g) at equilibrium; q_t is the amount of dye adsorbed (mg/g) at time, (t), K_{ad} is the rate constant of adsorption, (1/min) and t is agitation time (min.)

Linear plots of log (q_e-qt) Vs t show the applicability of the above model [Fig.4a]. The K_{ad} values have been calculated from the slope of the linear plots and are represented in Table 1 for different concentrations of the dyes studied. The rate constants observed are comparable with the values reported earlier [30].Diffusive transport through the internal pores of the nanocomposites and/or along the pore–wall surface (intraparticle diffusion) adsorption or attachment of the solute particle at a suitable site on the nanoparticle surface one or more of the above steps may be the rate controlling factor.

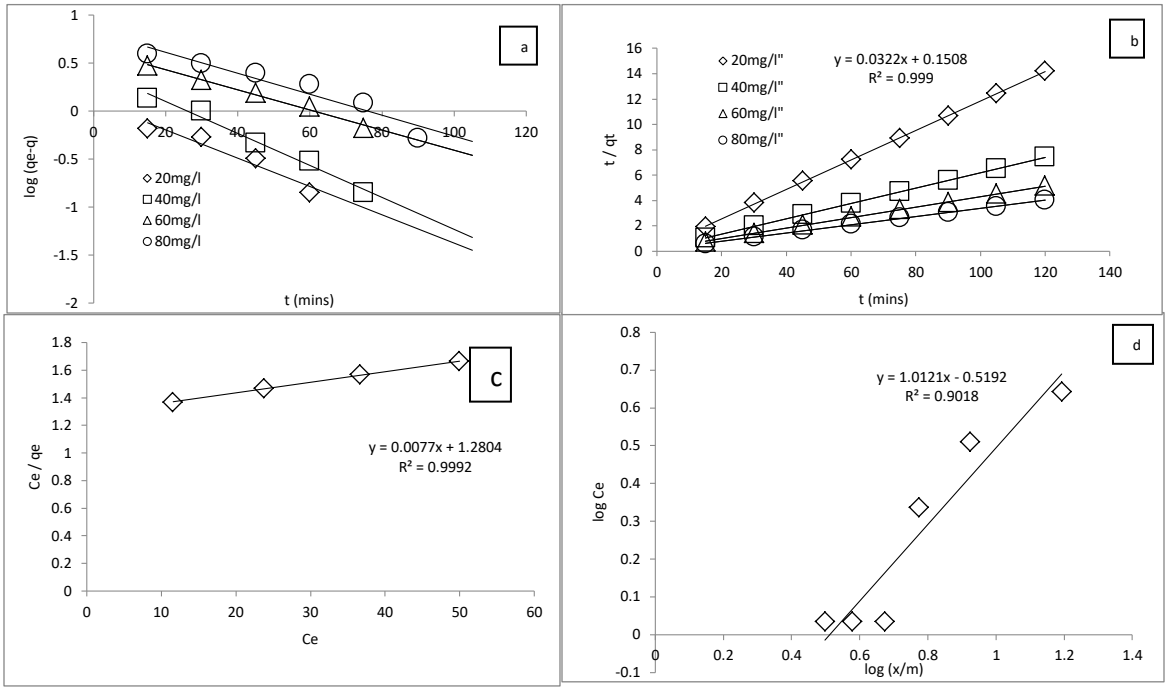

Fig.4. Adsorption isotherm models (a) Pseudo first order (b) Pseudo 2nd order,(c) Langmuir (d) Freundlich isotherm

3.3.2. Pseudo-second-order model

The pseudo-second-order model is represented by the following differential equation:

$$dq_t/dt = k_2 (q_e-q_t)^2 \qquad (2)$$

where q_e = Amount of dye adsorbed (mg/g at equilibrium),q_t = amount of dye adsorbed (mg/g at time t) k^2 is the equilibrium rate constant of pseudo-second order (g/mg/min) adsorption. Integrating the above equation for the boundary condition t = 0 to t and q_t = 0 to q, gives:

$$\mathbf{t/q = 1/k_2q_e^2 + 1/q_e \,.\, t} \qquad (3)$$

The slope and intercept of plot of t/q versus t were used to calculate the second-order rate constant k^2 (Fig.4b, Table 1). The correlation coefficients of all examined data were found very high which showed that the model can be applied for the entire adsorption process. From the figure it can be concluded that pseudo-second-order model was the best fit for the experimental data at different initial methylene blue concentrations. This suggested that the adsorption of RB may be due to electrostatic attraction between the charged surface and charged dyes molecules and may be inclined physisorption to a lesser extent and more towards chemisorption with increase in irradiation time [31].

3.3.3. Adsorption isotherm studies

The adsorption isotherms demonstrate the specific relation between the adsorption capacity of an adsorbent and the concentration of adsorbate at a constant temperature. The Langmuir and Freundlich isotherm models were used to study adsorption behavior of Methylene blue dye onto AC-SiO_2 nanocomposite.

3.3.3.1. Langmuir and Freundlich isotherms

Langmuir isotherm can be expressed as

$$q_e = \{(Q_0 \text{ x } b \text{ x } C_e) / (1 + (b \text{ x } C_e)\} \qquad (4)$$

where Q_0 is the maximum adsorption capacity per adsorbent mass (mg g^{-1}) and b is a constant related to the adsorption energy (L mg^{-1}). The Freundlich adsorption equation model is expressed by

$$q_e = K_f Ce^{1n} \qquad (5)$$

where K_f and 1/n are the Freundlich constants, and K_f represents the relative adsorption capacity of the adsorbent and n represents the adsorption dependence on equilibrium concentration of methylene blue. The slopes of the linear form of Langmuir and Freundlich plots [Fig.4c & 4d] were used to determine the adsorption constants tabulated in Table 1. In the present investigation, the value of R_L was less than one which showed that the adsorption process was favorable [29]. The regression coefficients show that the

adsorption data has a better fit to Langmuir than to the Freundlich isotherm which may be due to the monolayer coverage of the dye on the AC-SiO_2 nanocomposite. However, as the process is multistage process the data fit well into both the isotherm models.

Table 1. Pseudo first order, second order, Langmuir and Freundlich constants for Rhodamine B onto AC-SiO_2 nanocomposite

Conc (ppm)	Pseudo first order	Pseudo second order			Freundlich			Langmuir		
	K_{ad} (min^{-1})	K_2	h	R^2	R^2	K_f	n	Q_o	b	R^2
20	3.40844	298.94	4.022526	0.9998	0.9018	0.3025	0.9880	129.8	166.2	0.9992
40	3.84601	2126.11	7.782101	0.9999	0.9053	0.4998	1.1003			
60	2.41815	3557.58	6.097561	0.9995	0.9177	1.2615	1.4357			
80	2.5333	6395.68	6.6313	0.999	0.9588	3.1067	1.8839			

The Freundlich model describes a reversible adsorption on heterogeneous surfaces of the adsorbent and it is consistent with a multilayer adsorption of methylene blue on the Ac-SiO_2 structure.

3.3.3.2. Elovich equation.

The simple Elovich model equation is generally expressed by the following equation

$$q_t = \alpha + \beta \ln t \quad (6)$$

The slope and intercept of plot of qt Vs. ln t were used to calculate the values of the constants 'a' and 'b' as shown in

[Fig. 5a] and the constants are tabulated in Table 2.

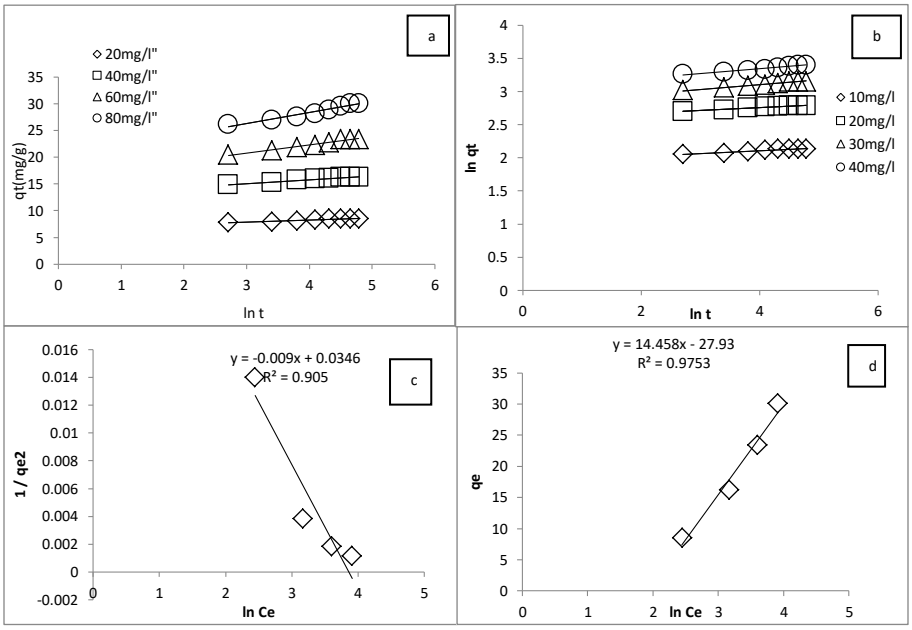

Fig. 5. Adsorption isotherm models (a) Elovich (b) fractional power model (c) Harkins Jura (d) Tempkin isotherm

3.3.3.4. Fractional power model

The fractional power model is a modified form of the Freundlich equation and can be expressed as:

$$\ln q_t = \ln a + b \ln t \quad (7)$$

where q_t the amount of the dyes sorbed by the adsorbent at time't' and 'a' and 'b' are constants with b < 1. The function 'a' 'b' is also a constant, being the specific sorption rate at unit time, i.e., when t = 1. The plot of ln t vs ln q_t showed the linear relationship and the computed constants 'a' and 'b' from the intercepts and slopes of the plots are presented in Fig. 5b. Table 2.

3.3.3.5. Harkin's–Jura adsorption isotherm.

This can be expressed as

$1/q_e^2 = (B/A) - (1/A) \log C_e$ (8)

where B and A are the isotherm constants. The Harkins–Jura adsorption isotherm accounts to multilayer adsorption and can be explained with the existence of a heterogeneous pore distribution. $1/q_e^2$ was plotted Vs. log Ce [Fig.5c, Table 2].

Table.2. Elovich, Fractional power model, Harkins Jura plot and Tempkin model constants for Methylene blue adsorption onto AC-SiO_2 nanocomposite

Model	Constants			
Elovich	**Conc (ppm)**	**α**	**β**	**R^2**
	20	6.7784	0.3641	0.9384
	40	12.922	0.7165	0.9652
	60	16.134	1.5354	0.9758
	80	20.207	2.0313	0.954
Fractional Power	**Conc (ppm)**	**a**	**b**	**R^2**
	20	6.881248	0.0447	0.9396
	40	13.12869	0.046	0.964
	60	16.82389	0.0699	0.9798
	80	21.18514	0.0724	0.9613
Harkin's Jura	**R^2**	**A**	**B**	
	0.905	111.111	3.84444	
Tempkin	**a**	**b**	**p**	
	0.14489	14.458	172.5135	

3.3.3.6. Tempkin model

The Tempkin isotherm equation is given as

$$q_e = RT/b \ln (KTC_e) \quad (9)$$

or

$$q_e = B \ln KT + B \ln C_e \quad (10)$$

Where A = KT; B = RT/b, T is the absolute temperature in K, R is Universal gas constant, 8.314 J/mol/ K, KT the equilibrium binding constant (l/mg) and B is related to the heat of adsorption [32]. A plot of q_e versus ln C_e at studied temperature is given in Fig.5d. The constants obtained for Tempkin isotherm are shown in Table 2. The Tempkin constant B shows that the heat of adsorption decreases with the increase in temperature, indicating exothermic adsorption [33]. A uniform distribution of binding sites on the nanocomposite surface was also confirmed by the Tempkin isotherm.

4. CONCLUSION

AC/SiO_2 composites were synthesized using microwave assisted sol-gel method and we have studied the possibility of using the nanocomposite for degradation of the cationic dye, Methylene blue and was found to be feasible under adequate and proper experimental conditions. The studies showed that 90% of the dye could be removed. The kinetics better fitted to pseudo second-order and the Freundlich model best described equilibrium data. The process is endothermic. It could improve the photo catalyst reaction efficiency to 90% within two hours .It has been considered that the large specific surface area, increase of •OH radicals, decreasing band gap energy and electron hole pair recombination have strong influence on the improvement of photocatalytic activity. The enhanced dye removal method brings photocatalysis a step closer to sustainable wastewater remediation methods. The combination of carbon and SiO_2, the formation of high surface area and mesoporous surfaces favor the methylene blue adsorption. The interaction between SiO_2 and carbon, as well as the carbon amount, is fundamental for preparing nanocomposites with appropriate characteristics for the wastewater treatment.

REFERENCE

[1] Wei, M. C.; Wang, K.S.; Huang, C.L.; Chiang, C.W.; Chang, T.J.; Lee, S.S.; Chang, H. (2012): Improvement of Textile Dye Removal by Electrocoagulation with Low-Cost Steel Wool Cathode Reactor. Chem. Eng. J., **192**, pp. 37–44.

[2] Bibak, O.; Aliabadi, M. (2014):Photocatalytic degradation of malachite green in aqueous solution using TiO_2 nanocatalyst, *J. Bio. & Env*,. *Sci*. ***5***, pp.301-310.

[3] Zhang, Y. C.; Li, J.; Zhang, M.; Dionysiou, D.(2011): Size-tunable hydrothermal synthesis of SnS_2 nanocrystals with high performance in visible light-driven photocatalytic reduction of aqueous Cr(VI), *Environ. Sci. Technol*., ***45***, pp. 9324-9331.

[4] Kandula, S.; Jeevanandam, P. (2015):A facile synthetic approach for $SiO_2@Co_3O_4$ core–shell nanorattles with enhanced peroxidase-like activity, RSC Adv., **5**, pp.5295– 5306.

[5] Schaefer, C. G.; Vowinkel, S.; Hellmann, G. P.; Herdt, T.; Contiu, C.; Schneider, J. J.; Gallei, M.(2014): A polymer based and template-directed approach towards functional multidimensional micro-structured organic/inorganic hybrid materials, J. Mater. Chem., **2,** pp.7960–7975.

[6] Yuliati, L.; Tsubota, M.; Satsuma, A.; Itoh, H.; Yoshida, H. (2006): Photoactive sites on pure silica materials for nonoxidative direct methane coupling, J. Catal., **238**, pp.214–220.

[7] Bal, R.; Tope, B. B.; Das, T. K.; Hegde, S. G.; Sivasanker, S. (2001): Alkali loaded silica, a solid base: investigation by FTIR spectroscopy of adsorbed CO_2 and its catalytic activity, J. Catal., **204**, pp.358-363.

[8] Senthilvelan, S.; Chandraboss, V. L.; Karthikeyan, B.; Natanapatham, L.; Murugavelu, M. TiO_2, (2013). ZnO and nanobimetallic silica catalyzed Photodegradation of methyl green, Mater. Sci. Semicond. Process., **16**, pp.185–192.

[9] [Chandraboss V.L; Senthilvelan, S.;Natanapatham,L.;Murugavelu,M.;Loganathan,B. ;Karthikeyan,B. **(2013)** Photocatalytic effect of Ag and Ag/Pt doped silicate non crystalline material on methyl violet–Experimental and theoretical studies, J. Non-Cryst. Solids, **368**, pp.23–28.

[10] Tsumura, T.; Kojitani, N.; Umemura, H.; Toyoda, M.; Inagaki, M.(2002): Composites between photoactive anatase-type TiO_2 and adsorptive carbon. *Appl Surf Sci*., ***196***, pp.429–436.

[11] Velasco, L. F.; Parra, J. B.; Ania, C. O. (2010): Role of activated carbon features on the photocatalytic degradation of phenol, *Appl. Surf. Sci*., ***256***, pp.5254–5258.

[12] Loganathan, B.; Chandraboss, V.L.; Murugavelu, M.; Senthilvelan, S.; Karthikeyan, B.(2015): Synthesis and characterization of multimetallic-core and siliceous shell $Au/Pt/Ag@SiO_2$ sol–gel derived nanocomposites, J. Sol-Gel Sci. Technol., **74**, pp.1- 14.

[13] Andriantsiferana, C.; Mohamed E. F.; Delmas, H. (2013) Photocatalytic degradation of an azo-dye on TiO_2/activated carbon composite material, Environ. Technol. 2013, DOI:10.1080/09593330.2013.828094.

[14] Pozzo, R. L.; Baltan, M. A.; Cassano, A. E. (1997): Supported titanium oxide as photocatalyst in water decontamination: state of the art. Catal Today., **39**, pp. 219–231.

[15] Selhan Karago¨z,, Turgay Tay , Suat Ucar , Murat Erdem.(2008): Activated carbons from waste biomass by sulfuric acid activation and their use on methylene blue adsorption. Bioresource Technology, **99,** pp. 6214–6222

[16] Jinlong Li, Deshuai Zhen, Guozhe Sui, Chunming Zhang, Qigang Deng, and Lihua Ji.(2012): Nanocomposite of $Cu–TiO_2–SiO_2$with high photoactive performance for degradation of Rhodamine B dye in aqueous wastewater. Journal of Nanoscience and Nanotechnology.**12**, pp.6265–6270.

[17] Mahesh, K.P.O.; Kuo, D.H.; Huang B.R.(2015): Facile synthesis of hetero structured Ag-deposited $SiO_2@TiO_2$ composite spheres with enhanced catalytic activity towards the photodegradation of AB1 ye, J. Mol. Catal. A: Chem. **396**, pp. 290-296.

[18] Wang, X.;. Xi, M.; Wang, X.; Fong, H.; Zhu, Z.(2016): Flexible composite felt of electrospun TiO_2 and SiO_2 nanofibers infused with TiO_2 nanoparticles for lithium ion battery anode, Electrochim. Acta, **190,** pp. 811-816.

[19] Dariania,R.S.;Esmaeilia,A.;Mortezaalia,A.; Dehghanpour,S.(2016):Photocatalytic reaction and degradation of methylene blue on TiO_2 nano-sized particles .Optik, **127,** pp. 7143–7154

[20] Ling, C.; Mohamed, (2004): Photo degradation of methylene blue dye in aqueous stream, J. Technol. **40,** pp. 91–103.

[21] Ghorai, S.; Sarkar, A.; Raoufi,; Panda, A. B.; Schönherr, H.; Pal, S.(2014): *ACS app. mater. & interfaces*. **6,** pp. 4766-4777

[22] Hesham Fouad Aly, Ahmed Ibrahim Abd-Elhamid.(2018): Photocatalytic degradation of Methylene blue dye Using Silica oxide nanoparticles as a catalyst.Water Environment Research,**9**, pp. 807-818.

[23] Matthews, R.W.(1989): Photocatalytic oxidation and adsorption of Methylene blue on thin films of near – UV illuminated TiO. J. Chem. Soc. Fara. Trans., **85,** pp. 1291–302..

[24] Dongen Zhang, Jinbo Wu, Bingpu Zhou, Yaying Hong, Shunbo Lia and Weijia Wen. Efficient photocatalytic activity with carbon-doped SiO_2 nanoparticles, Nanoscale, DOI: 10.1039/c3nr01314f.

[25] Chen, D.; Rey, A.K, (1999): Photocatalytic kinetics of phenol and its derivatives over UV irradiated TiO_2. Appl. Catal. B: Environ.. **23** (2–3), pp.143–157.

[26] Ranjith, R.; Shameela Rajam,P.(2017): Removal of cationic dyes from aqueous solution by adsorption on mesoporous TiO_2-SiO_2. J. Nanosci. Tech., **3**(3), pp. 273–280.

[27] Balachandran.; Rajendran Venckatesh.; Rajeshwari Sivaraj.;Rajiv,P.(2014): TiO_2 nanoparticles versus TiO_2–SiO_2 nanocomposites: A comparative study of photo catalysis on acid red 88. Spectrochimica Acta Part A: Molecular and Biomolecular Spectroscopy, **128,** pp. 468–474.

[28] Pugacheskii, M.A.(2013): Photocatalytic properties of titania nanoparticles obtained by laser ablation. Nanotechnol. Russ., **8** (7–8), pp. 432–436.

[29] Ghaedi,M.; Ghaedi, A.M.; Hossainpour, M.; Ansari,A.; Habibi,M.H. Asghari,A.(2014): Least square-support vector (LS-SVM) method for modeling of Methylene blue dye adsorption using copper oxide loaded on activated carbon: Kineti and isotherm study Ind. Eng. Chem. Res. **20**(4), pp.1641-1649.

[30] Chaudhuri,H.; Dash, S.; Sarkar, A.(2016): Adsorption of different dyes from aqueous solution using Si-MCM-41 having very high surface area. J. Porous Mater., **23**(5), pp.1227-1237.

[31] Hazzaa,R.;Hussein, M.(2015): Adsorption of cationic dye from aqueous solution onto activated carbon prepared from olive stones. Environ. Technol. Innovat., **4,** pp. 36-51.

[32] Foo, K.Y. (2012): Preparation, characterization and evaluation of adsorptive properties of orange peel based activated carbon via microwave induced K_2CO_3 activation. Bioresour. Technol., 104, pp.679–686.

[33] Wang, X.S; Qin, Y.(2005): Equilibrium sorption isotherms for of Cu^{2+} on rice bran. Process Biochem.,**40**, pp. 677–680.